European Review for Medical and Pharmacological Sciences 2019; 23: 7786-7801

Critical analysis of major and ancillary features of LI-RADS v2018 in the differentiation of small (≤ 2 cm) hepatocellular carcinoma from dysplastic nodules with gadobenate dimeglumine-enhanced magnetic resonance imaging

A.M. DE GAETANO[1,2], M. CATALANO[1,2], M. POMPILI[3,4], M.G. MARINI[1,2], P. RODRÍGUEZ CARNERO[5], C. GULLÌ[1,2], A. INFANTE[1], R. IEZZI[1,2], F.R. PONZIANI[3], L. CERRITO[3], G. MARRONE[3], F. GIULIANTE[6], F. ARDITO[6], G.L. RAPACCINI[7], F.M. VECCHIO[8], L. GIRALDI[9], R. MANFREDI[1,2], HEPATOCATT STUDY GROUP

[1]Department of Diagnostic Imaging, Oncological Radiotherapy and Hematology, Fondazione Policlinico Universitario Agostino Gemelli – IRCCS, UOC di Radiologia, Rome, Italy
[2]Università Cattolica del Sacro Cuore, Istituto di Radiologia, Rome, Italy
[3]Department of Gastroenterological, Endocrine-Metabolic and Nephro-Urological Sciences, Fondazione Policlinico Universitario Agostino Gemelli – IRCCS, UOC di Medicina Interna e Gastroenterologia, Rome, Italy
[4]Università Cattolica del Sacro Cuore, Istituto di Medicina Interna e Geriatria, Rome, Italy
[5]Department of Radiology, Hospital Universitario de la Princesa, Madrid, Spain
[6]Department of Gastroenterological, Endocrine-Metabolic and Nephro-Urological Sciences, Fondazione Policlinico Universitario Agostino Gemelli – IRCCS, UOC di Chirurgia Generale ed Epatobiliare, Università Cattolica del Sacro Cuore, Rome, Italy
[7]Department of Gastroenterological, Endocrine-Metabolic and Nephro-Urological Sciences, Fondazione Policlinico Universitario Agostino Gemelli – IRCCS, UOC di Medicina Interna e Gastroenterologia Columbus, Università Cattolica del Sacro Cuore, Rome, Italy
[8]Department of Gastroenterological, Endocrine-Metabolic and Nephro-Urological Sciences, Fondazione Policlinico Universitario Agostino Gemelli – IRCCS, UOC di Anatomia Patologica, Università Cattolica del Sacro Cuore, Rome, Italy
[9]Department of Hygiene, Institute of Public Health, Università Cattolica del Sacro Cuore, Rome, Italy

Abstract. – OBJECTIVE: To evaluate the performance of major features, ancillary features, and categories of Liver Imaging Reporting and Data System (LI-RADS) version 2018 at magnetic resonance (MR) imaging in the differentiation of small hepatocellular carcinoma (HCC) from dysplastic nodules (DNs).

PATIENTS AND METHODS: This retrospective study included cirrhotic patients with pathologically proven untreated HCCs and DNs (≤ 2 cm) and liver MR imaging performed with gadobenate dimeglumine contrast agent within 3 months before pathological analysis, between 2015 and 2018. 37 patients with 43 observations (17 HCCs and 26 DNs) met the inclusion criteria. Two radiologists assessed major and ancillary imaging features for each liver observation and assigned a LI-RADS v2018 category in consensus. Estimates of diagnostic performance of major features, ancillary features, and LI-RADS categories were assessed based on their sensitivity, specificity, positive (PPV), and negative predictive values (NPV).

RESULTS: Major features (nonrim arterial phase hyperenhancement, nonperipheral "washout", and enhancing "capsule") had a sensitivity of 94.1%, 88.2%, and 41.2%, and a specificity of 57.7%, 42.3%, and 88.5% for HCC, respectively. Ancillary features (hepatobiliary phase hypointensity, mild-moderate T2 hyperintensity, restricted diffusion, and fat in the lesion more than adjacent liver) had a sensitivity of 94.1%, 64.7%, 58.8%, and 11.8%, and a specificity of 26.9%, 61.5%, 65.4%, and 76.9% for HCC, respective-

Corresponding Author: Marialavinia Catalano, MD; e-mail: marialavinia.catalano@gmail.com

ly. The LR-5 category (determined by using major features only vs. the combination of major and ancillary features) had a sensitivity of 88.2% at both evaluations and a specificity of 76.9% and 80.8% for HCC, respectively. The combination of LR-4, LR-5 categories (determined by using major features only vs. the combination of major and ancillary features) had a sensitivity of 94.1% at both interpretations and a specificity of 65.4% and 26.9% for HCC, respectively. The use of ancillary features modified LI-RADS category in 25.6% of observations (11/43), predominantly upgraded from LR-3 to LR4 (10/11), increasing the proportion of low-grade DNs and high-grade DNs categorized as LR-4 (from 15.4% to 61.5% and from 7.7% to 46.1%, respectively).

CONCLUSIONS: The added value of ancillary features in combination with major features is limited for the non-invasive diagnosis of small HCC; however, their use modifies the final category in a substantial proportion of observations from LR-3 to LR-4, thus allowing possible changes in the management of patients at risk for HCC.

Key Words:

Hepatocellular carcinoma (HCC), Dysplastic nodules (DNs), Magnetic Resonance Imaging (MRI), LI-RADS (Liver Imaging Reporting and Data System), Major imaging features, Ancillary imaging features.

Introduction

Hepatocellular carcinoma (HCC) is the most frequent primary liver malignant neoplasm, the second leading cause of cancer mortality worldwide, and a major cause of death in patients with cirrhosis[1]. Most HCCs develop through hepatocarcinogenesis, a multistep process where dysplastic nodules (DNs), which are about 1-1.5 cm in diameter[2], represent a key stage having histological features suggestive of a clonal cell population, and can be divided into low and high grade (LGDNs and HGDNs) based on their architectural and cellular atypia. HGDNs are premalignant lesions; early HCCs (E-HCCs) are considered "carcinoma *in situ*"; in contrast, progressed HCCs (P-HCCs) are overt malignancies that can invade vessels and metastasize[3,4]. The differentiation of small (≤ 2 cm) HCC from DNs is pivotal in the management of cirrhotic patients as only HCCs are considered malignant lesions to be treated[5-7]. Unlike most other cancers, HCC can be diagnosed noninvasively with imaging without pathology confirmation[5-7]. Nowadays, many diagnostic systems provide algorithms and criteria for imaging-based diagnosis of HCC[8], and among these, the Liver Imaging Reporting and Data System (LI-RADS), firstly released in 2011 and supported by the American College of Radiology (ACR) represents a radiology-driven and multidisciplinary collaborative categorization system aimed at standardizing performance of liver imaging in patients with or at risk for HCC, as well as interpretation and reporting of the results. With the changes introduced in the last update in 2018[9], LI-RADS was integrated into the most recent HCC clinical practice guidance by the American Association for the Study of Liver Disease (AASLD)[10], due to the evidence that its categories accurately stratify the probability of HCC and overall malignancy[11]. This represented a major step toward establishing a universal approach to the imaging diagnosis of HCC and further solidified the role of radiologists in this process[9].

LI-RADS assigns categories that reflect the relative probability of benignity, HCC, or other malignancy to detect untreated liver observations based on the presence of major and ancillary imaging features. Categories include LR-1 (definitely benign), LR-2 (probably benign), LR-3 (intermediate probability of malignancy), LR-4 (probably HCC), LR-5 (definitely HCC), LR-TIV (definite tumor in vein), and LR-M (probably or definitely malignant, not specific for HCC)[9]. MR imaging is often used for the non-invasive diagnosis of HCC as it provides considerable tissue contrast and is the only modality that can assess all major and ancillary imaging features[9]. In LI-RADS lexicon, major features refer to the five imaging features included in the diagnostic table for categorizing LR-3, LR-4, and LR-5 observations[12]. These features refer to nonrim arterial phase hyperenhancement (nonrim APHE), nonperipheral "washout", enhancing "capsule", size, and threshold growth. In contrast, ancillary features are divided in those favoring benignity, those favoring malignancy in general, and those favoring HCC in particular. Their use is optional, thus, unlike major features, ancillary features are applied at the radiologist's discretion, and may be used to improve detection or characterization, increase confidence, or adjust observation category, by up- or downgrading a category by one; however, they cannot be used to upgrade to LR-5, to preserve high specificity of this category[9].

The diagnostic performance of LI-RADS categories has been previously assessed[13,14]; also the accuracy of major features for the diagnosis of HCC has been widely evaluated[15-18]. Neverthe-

less, this has not been the case for most ancillary features, indeed previous papers have included these features as part of sets of diagnostic criteria and few have reported their individual diagnostic performance at MR imaging[17-19]. Furthermore, even though several previous works[20-22] have suggested that LI-RADS ancillary features may be helpful in differentiating hepatocellular nodules, the precise characterization can be complex and challenging, especially for small nodules, particularly because DNs and E-HCCs can show overlapping imaging findings[23-25]; in addition, the added value of ancillary features in LI-RADS categorization appears controversial according to recent studies[26,27] assessing their clinical application. Thus, there is the need to assess the impact of ancillary features on major feature-determined LI-RADS category and to assess the value of their application in the diagnosis of HCC in at-risk patients. This study aimed to evaluate the performance of major features, ancillary features, and LI-RADS v2018 categories at MR imaging for the differentiation of small HCCs from DNs, and to assess the impact of the use of ancillary features on LI-RADS v2018 categorization.

Patients and Methods

Patients

In this institutional review board-approved single-site study, we retrospectively reviewed our MR imaging database for cirrhotic patients with pathologically proven ≤ 2 cm lesions, including both DNs and HCCs diagnosed at Fondazione Policlinico Universitario A. Gemelli – IRCCS, Rome. We strictly evaluated patients with liver MR imaging performed within 3 months before the pathological analysis. We excluded all the patients with prior history and/or systemic treatment of HCC, all the observations that had been previously treated percutaneously, and all the observations without pathologic confirmation. All MR exams were performed in our institution with our routine protocol for the study of focal liver lesions in patients at risk of HCC. We excluded all the patients with MR imaging of insufficient quality for diagnosis or performed without hepatobiliary contrast agents. Between January 2015 and January 2018, 37 cirrhotic patients with a total of 43 observations (29 men, 8 women; mean age 64 years ± 10) met inclusion criteria. Characteristics of patients and observations included in the final study cohort are summarized in Table I.

Table I. Characteristics of patients, observations, and tests included in study cohort.

Characteristic	Data
Patients	37
Sex	
Male	29 (78%)
Female	8 (22%)
Age (y)	
Mean ± Standard Deviation	64.0 ± 10.2
Etiology of Cirrhosis	
Hepatitis C Infection	14/37 (38%)
Hepatitis B Infection	3/37 (8%)
Alcoholic Liver Disease	11/37 (30%)
Nonalcoholic Steatohepatitis	3/37 (8%)
Primary Biliary Cholangitis	1/37 (3%)
Primary Sclerosing Cholangitis	1/37 (3%)
Hemochromatosis	2/37 (5%)
Cryptogenetic	2/37 (5%)
Alpha-fetoprotein	
< 200 ng/ml	36/37 (97%)
> 200 ng/ml	1/37 (3%)
Observations	43
HCC	17/43 (40%)
Early HCC	6/43 (14%)
Progressed HCC	11/43 (26%)
DN	26/43 (60%)
Low grade DN	13/43 (30%)
High grade DN	13/43 (30%)
Size (mm)	
Mean ± Standard Deviation	15.3 ± 3.5
Range	9-20
HCC	
Mean ± Standard Deviation	15.8 ± 3.1
DN	
Mean ± Standard Deviation	15.3 ± 3.8
Reference Standard	
FNB/CNB	23/43 (53.5%)
Hepatectomy	16/43 (37.2%)
Liver Explant	4/43 (9.3%)
Time interval between index MR imaging and pathologic analysis as reference standard (d)	
Mean ± Standard Deviation	49.0 ± 28.5

Note: Unless otherwise specified, data are numerators and denominators, and data in parenthesis are percentages. HCC = hepatocellular carcinoma, DN = dysplastic nodule, FNB = fine needle biopsy, CNB = core needle biopsy, LI-RADS = Liver Imaging Reporting and Data System.

The diagnosis of cirrhosis was made using histological and/or clinical findings (laboratory and/or imaging parameters). Histopathologic analysis for each observation, which occurred 1 day to 3 months after the index MR examination, was the diagnostic reference standard. The histological diagnosis was provided by fine-needle biopsy (FNB) or core-needle biopsy (CNB) specimens (*n = 23*), by hepatectomy (*n = 16*) and explants

specimens ($n = 4$), and it was made according to the International Consensus Group for Hepatocellular Neoplasia[4]. There were 17 HCCs (6 well-differentiated E-HCCs and 11 P-HCCs, respectively) and 26 DNs (13 LGDNs and 13 HGDNs, respectively). All observations were ≤ 2 cm in size (mean size 1.53 cm [1.58 cm for HCCs, 1.53 cm for DNs]).

Liver MR Imaging Protocol

Liver MR imaging was performed with 1.5 Tesla system [Signa Horizon, General Electric (GE) Healthcare, Milwaukee, WI, USA] with our routine protocol for the study of focal liver lesions in patients at risk of HCC, including dynamic contrast-enhanced imaging performed after the administration of gadobenate dimeglumine. MR imaging technique is summarized in Table II.

Image Analysis

Two board-certified radiologists, experienced in the interpretation of liver MR imaging (15 and 5 years of experience in abdominal imaging, respectively), blinded to the pathologic result, retrospectively reviewed the MR images in consensus and were informed of the exact location of each nodule before imaging interpretation.

Readers assessed the presence or absence of all major and ancillary imaging features for each liver observation and assigned a LI-RADS category in consensus. Assessment of observation categories based on LI-RADS v2018[9] was performed first, according to the algorithm based on major imaging features only, and second, the assessment was provided based on major and ancillary features in combination. When a feature could not be assessed (for example, threshold growth could not be evaluated in a patient without previous imaging examinations), then it was considered not applicable. To assess the added value of ancillary features, the readers were allowed to adjust (upgrading or downgrading) observation category based on the presence of at least one ancillary feature; however, they were not allowed to adjust category in case of conflicting ancillary features (i.e., one or more favoring malignancy and one or more favoring benignity), and were not allowed to upgrade LR-4 to LR-5 to preserve high specificity for HCC with LR-5 category, as specified by LI-RADS rules for the application of the ancillary features[9].

Statistical Analysis

Categorical variables were expressed as numbers and percentages; continuous variables were expressed as means ± standard deviations. Estimates of diagnostic performance of major features, ancillary features, and LI-RADS categories were assessed based on their sensitivity, specificity, positive (PPV), negative predictive values (NPV), and likelihood ratios (LR), and expressed with 95% confidence intervals. The number and percentages of HCCs and DNs in each LI-RADS category were documented at interpretation before and after the use of ancillary features. The number and proportion of observations in which the use of ancillary features modified the final LI-RADS category were calculated. The relationship between obser-

Table II. MR Imaging protocol.

Sequence	FS	TR/TE (ms)	FA	ST (mm)	SS (mm)	FOV (cm)	Matrix
Baseline							
T1-w 2D FSPGR							
In-phase	No	160/4.8-2.3	60°	5	1	48×48	288×224
Out of-phase	No	160/4.8-2.3	60°	5	1	48×48	288×224
T2-w SSFSE	No	1500/100	90°	5	1	48×48	320×224
T2-w SSFSE							
Transverse	Yes	1500/100	90°	5	1	48×48	320×224
Coronal	No	1500/100	90°	5	0	48×48	320×224
Dynamic							
T1-w 3D FSPGR	Yes	4.6/2.1	12°	4	0	48×48	320×224
DWI	Yes	4500/79.2	90°	5	1	40×40	96×128

Note: FS = fat suppression, TR = repetition time, TE = echo time, FA = flip angle, ST = slice thickness, SS = slice spacing, FOV = field of view, T1/T2-w = weighted, SSFSE = single-shot fast spin-echo, FSPGR = fast spoiled gradient-echo. Dynamic contrast enhanced imaging was performed after the administration of hepatobiliary contrast agent (gadobenate dimeglumine). Imaging was obtained in the pre-contrast, arterial (≈30 s), portal venous (≈60 s), equilibrium phase (≈180 s), and hepatobiliary phase (≈ 90-120 min). A free-breathing single-shot echo-planar diffusion-weighted sequence was acquired at b-values 0 and 800 s/mm^2 before contrast agent infusion.

vations MR imaging features and histological classification was analyzed by Fisher's exact test. All analyses were performed on a per-lesion basis. A *p*-value less than 0.05 was considered statistically significant. All statistical analyses were performed using Stata software (StataCorp. 2015. Stata Statistical Software: Release 14. College Station, TX, USA: StataCorp LP).

Results

Characteristics of Observations

A total of 43 index observations were included in this study. Characteristics of observations including size, reference standard, final diagnosis, and the time interval between index test and reference standard are summarized in Table I. All observations were ≤ 2 cm with a mean size of 1.53 cm. The mean size of HCCs and DNs assessed in this study was 1.58 cm and 1.53 cm, respectively. Table III shows MR imaging features of observations assessed in the final study cohort. LI-RADS categorization of observations – according to major features only and according to ancillary features in combination with major features – is summarized in Table IV.

Diagnostic Performance of Major Features

Table Va shows the diagnostic performance parameters for major imaging features according to the LI-RADS v2018 algorithm. Per-lesion sensitivity of major features for HCC ranged from 41.2% to 94.1% and was highest for nonrim APHE. Per-lesion specificity of major features ranged from 42.3% to 88.5% and was highest for enhancing "capsule". Per-lesion PPV of major features ranged from 50% to 70% and was highest for enhancing "capsule". Estimates of diagnostic performance of threshold growth could not be computed because this feature was too infrequent or was not assessable for a substantial number of observations. Estimates of diagnostic performance of observation size were not assessed as we strictly included ≤ 2 cm observations in our study.

Diagnostic Performance of Ancillary Features in Favor of Malignancy or HCC

The diagnostic performance parameters for ancillary features in favor of malignancy – or HCC in particular – are summarized in Table Vb. Per-lesion sensitivity of ancillary features in favor of malignancy – or HCC in particular – ranged from 11.8% to 94.1% and was highest for the hepatobiliary phase (HBP) hypointensity. Per-lesion specificity of ancillary features in favor of malignancy – or HCC in particular – ranged from 26.9% to 76.9% and was highest for fat in mass. Per-lesion PPV of ancillary features in favor of malignancy – or HCC in particular – ranged from 25% to 52.6% and was highest for restricted diffusion. Estimates of diagnostic performance could not be computed for subthreshold growth, corona enhancement, fat sparing, and iron sparing in solid mass, as these features were too infrequent. Transitional phase hypointensity was not included in the evaluation of ancillary features favoring malignancy due to the exclusive use of gadobenate dimeglumine as paramagnetic contrast agent. Estimates of diagnostic performance could not be performed for further ancillary features favoring HCC in particular (such as non-enhancing "capsule", nodule-in-nodule appearance, mosaic architecture, and blood products in mass), as well for ancillary features in favor of benignity because of the small number of observations displaying these features.

Diagnostic Performance of LI-RADS v2018 Categories

Table VI shows the diagnostic performance parameters for stratified LI-RADS categories according to major features only and in combination with ancillary features. The per-lesion sensitivity and specificity of LR-5 category for HCC were 88.2% and 76.9% when considering major features only. The per-lesion sensitivity and specificity of LR-5 were similar – 88.2% and 80.8%, respectively – when considering major features in combination with ancillary features. The per-lesion sensitivity and specificity of the combination of LR-4 and LR-5 for HCC were 94.1% and 65.4% when considering major features only, and 94.1%-26.9% with the use of ancillary features in combination with major features. Thus, when considering the combination of LR-4 and LR-5, the per-lesion sensitivity for HCC increased for both interpretations; however, the specificity decreased, and notably, was markedly lower for interpretation that included ancillary features.

LI-RADS Classification and Impact of Ancillary Features on Observation Categories

LI-RADS categorization of observations – according to major features only and according to ancillary features in combination with

Table III. MR imaging features of observations.

MR imaging features	HCC (n = 17)	DN (n = 26)	*p*-value	LGDN (n = 13)	HGDN (n = 13)	Early HCC (n = 6)	Progressed HCC (n = 11)	*p*-value
Nonrim APHE	16 (94.1%)	11 (42.3%)	0.001	4 (30.8%)	7 (53.8%)	6 (100.0%)	10 (90.9%)	0.004
Nonperipheral "washout"	15 (88.2%)	15 (57.7%)	0.045	7 (53.8%)	8 (61.5%)	5 (83.3%)	10 (90.9%)	0.190
Nonrim APHE + "washout"	15 (88.2%)	7 (26.9%)	< 0.001	1 (7.7%)	6 (46.1%)	5 (83.3%)	10 (90.9%)	< 0.001
Enhancing "capsule"	7 (41.2%)	3 (11.5%)	0.034	0 (0.0%)	3 (23.1%)	1 (16.7%)	6 (54.5%)	0.012
HBP hypointensity	16 (94.1%)	19 (73.1%)	0.119	9 (69.2%)	10 (76.9%)	5 (83.3%)	11 (100.0%)	0.265
HBP isointensity	1 (5.9%)	6 (23.1%)	0.215	3 (23.1%)	3 (23.1%)	1 (16.7%)	0 (0.0%)	0.306
Mild-moderate T2 hyperintensity	11 (64.7%)	10 (38.4%)	0.124	4 (30.8%)	6 (46.1%)	3 (50.0%)	8 (72.7%)	0.241
Restricted diffusion	10 (58.8%)	9 (34.6%)	0.209	4 (30.8%)	5 (38.5%)	0 (0.0%)	10 (90.9%)	0.001
Fat in mass	2 (11.8%)	6 (23.1%)	0.446	5 (38.5%)	1 (7.7%)	1 (16.7%)	1 (9.1%)	0.208

Note: APHE = Arterial Phase Hyperenhancement, HBP = Hepatobiliary Phase, *p* values for the evaluation of association of MR features and histological classification of observations (Fisher's exact Test).

7791

Table IV. Categorization according to LI-RADS v2018 algorithm and table (major features only) and categorization according to major and ancillary features.

Categorization According to LI-RADS v2018 Algorithm and Table (Major Features Only)					
	LR-3	LR-4	LR-5	LR-M	Total
HCC	0 (0.0%)	1 (5.9%)	15 (88.2%)	1 (5.9%)	17 (100.0%)
E-HCC	0 (0.0%)	1 (16.7%)	5 (83.3%)	0 (0.0%)	6 (100.0%)
P-HCC	0 (0.0%)	0 (0.0%)	10 (90.9%)	1 (9.1%)	11 (100.0%)
DN	16 (61.5%)	3 (11.5%)	6 (23.1%)	1 (3.9%)	26 (100.0%)
LGDN	9 (69.2%)	2 (15.4%)	1 (7.7%)	1 (7.7%)	13 (100.0%)
HGDN	7 (53.8%)	1 (7.7%)	5 (38.5%)	0 (0.0%)	13 (100.0%)
Categorization According to Major and Ancillary Features					
	LR-3	LR-4	LR-5	LR-M	Total
HCC	0 (0.0%)	1 (5.9%)	15 (88.2%)	1 (5.9%)	17 (100.0%)
E-HCC	0 (0.0%)	1 (16.7%)	5 (83.3%)	0 (0.0%)	6 (100.0%)
P-HCC	0 (0.0%)	0 (0.0%)	10 (90.9%)	1 (9.1%)	11 (100.0%)
DN	6 (23.1%)	14 (53.8%)	5 (19.2%)	1 (3.9%)	26 (100.0%)
LGDN	4 (30.8%)	8 (61.5%)	0 (0.0%)	1 (7.7%)	13 (100.0%)
HGDN	2 (15.4%)	6 (46.1%)	5 (38.5%)	0 (0.0%)	13 (100.0%)

Note: HCC = hepatocellular carcinoma, E-HCC = early hepatocellular carcinoma, P-HCC = progressed hepatocellular carcinoma, DN = dysplastic nodule, LGDN = low grade dysplastic nodule, HGDN = high grade dysplastic nodule.

major features – is summarized in Table IV. Taken together, most of the HCCs were categorized as LI-RADS category 5 (88.2% [15/17]) at both interpretations (i.e., before and after the application of the ancillary features); in particular, most of the E-HCCs (83.3% [5/6]) and most of the P-HCCs (90.9% [10/11]) were classified as LR-5. DNs were mostly classified as LR-3 (61.5% [16/26]), according to major features only, while they were mostly classified as LR-4 (53.8% [14/26]), according to ancillary features. In particular, at the interpretation according to major features only, LGDNs were predominantly classified as LR-3 (69.2% [9/13]), while, they were mostly categorized as LR-4 (61.5% [8/13]) at the interpretation that included ancillary features. HGDNs were frequently classified as LR-3 (53.8% [7/13]) at evaluation according to major features only, while they were frequently categorized as LR-4 (46.1% [6/13]) at the interpretation that included ancillary features. At both interpretations, a substantial proportion of HGDNs was categorized as LR-5 (38.5% [5/13]). In contrast, only 1 of 13 LGDNs was classified as LR-5 and the observation category was downgraded to LR-4 by using ancillary features.

Table VII illustrates the numbers and percentages of observation categories that were identical, upgraded or downgraded after application of ancillary features. The category of 74.4% of observations (32/43) was identical at both evaluations (according to major features only or according to the major features in combination with ancillary features). Among the 25.6% observations (11/43) that were modified by the application of ancillary features, the category was upgraded in 10 of 11 observations (90.9%) from LR-3 to LR-4, and downgraded in 1 of 11 observations from LR-5 to LR-4, with 66.7% of LR-4 observations (10/15) being upgraded from LR-3. All of the observations that were upgraded by using ancillary features in combination with major features were confirmed to be DNs at pathologic analysis (10/10, of which 5 were LGDNs, and 5 were HGDNs). According to the LI-RADS v2018 rules for the application of ancillary features, the observation category was upgraded in 10 of 16 observations (62.5%) eligible for category upgrade, with HBP hypointensity being the most frequently ancillary feature observed, as it was present in all of the upgraded observations (10/10). The category was downgraded in 1 of 41 observations (2.4%) eligible for category downgrade, due to the presence of HBP isointensity.

Figure 1 shows an example of HCC diagnosed based on major imaging features. Figures 2 and 3 illustrate two examples of liver observations in

Table V. Per-lesion diagnostic performance of major features according to algorithm and Table (a). Per-lesion diagnostic performance of ancillary features in favor of malignancy (b).

Major Features (a)	TP	TN	FP	FN	Sensitivity (%)	Specificity (%)	PPV (%)	NPV (%)	LR +
Nonrim APHE	16	15	11	1	94.1 (71.3-99.9)	57.7 (36.9-76.6)	59.3 (38.8-77.6)	93.8 (69.8-99.8)	2.22 (1.40-3.54)
Nonperipheral "washout"	15	11	15	2	88.2 (63.6-98.5)	42.3 (23.4-63.1)	50.0 (31.3-68.7)	84.6 (54.6-98.1)	1.53 (1.05-2.22)
APHE + Washout	15	19	7	2	88.2 (63.6-98.5)	73.1 (52.2-88.4)	68.2 (45.1-86.1)	90.5 (69.6-98.8)	3.28 (1.70-6.32)
Enhancing "capsule"	7	23	3	10	41.2 (18.4-67.1)	88.5 (69.8-97.6)	70.0 (34.8-93.3)	69.7 (51.3-84.4)	3.57 (1.07-11.90)
Features (b)	**TP**	**TN**	**FP**	**FN**	**Sensitivity (%)**	**Specificity (%)**	**PPV (%)**	**NPV (%)**	**LR +**
HBP hypointensity	16	7	19	1	94.1 (71.3-99.9)	26.9 (11.6-47.8)	45.7 (28.8-63.4)	87.5 (47.3-99.7)	1.29 (0.99 -1.67)
Mild-moderate T2 hyperintensity	11	16	10	6	64.7 (38.3-85.8)	61.5 (40.6-79.8)	52.4 (29.8-74.3)	72.7 (49.8-89.3)	1.68 (0.92-3.06)
Restricted diffusion	10	17	9	7	58.8 (32.9-81.6)	65.4 (44.3-82.8)	52.6 (28.9-75.6)	70.8 (48.9-87.4)	1.70 (0.88-3.29)
Fat in mass*	2	20	6	15	11.8 (1.5-36.4)	76.9 (56.4-91.0)	25.0 (3.2-65.1)	57.1 (39.4-73.7)	0.51 (0.12-2.40)

Note: Data in parenthesis are 95% confidence intervals. TP = true positive, TN = true negative, FP = false positive, FN = false negative, LR + = positive likelihood ratio, APHE = arterial phase hyperenhancement, HBP = hepatobiliary phase. *Ancillary feature that specifically favors hepatocellular carcinoma as opposed to malignancy in general.

Table VI. Per-lesion diagnostic performance of LI-RADS categories before and after application of ancillary features

According to major features only	TP	TN	FP	FN	Sensitivity (%)	Specificity (%)	PPV (%)	NPV (%)	LR +
LR-5	15	20	6	2	88.2 (63.6-98.5)	76.9 (56.4-91.0)	71.4 (47.8-88.7)	90.9 (70.8-98.9)	3.82 (1.86-7.88)
LR-4, LR-5	16	17	9	1	94.1 (71.3-99.9)	65.4 (44.3-82.8)	64.0 (42.5-82.0)	94.4 (72.7-99.9)	2.72 (1.58-4.67)
According to major and ancillary features	**TP**	**TN**	**FP**	**FN**	**Sensitivity (%)**	**Specificity (%)**	**PPV (%)**	**NPV (%)**	**LR +**
LR-5	15	21	5	2	88.2 (63.6-98.5)	80.8 (60.6-93.4)	75.0 (50.9-91.3)	91.3 (72.0-98.9)	4.59 (2.05-10.30)
LR-4, LR-5	16	7	19	1	94.1 (71.3-99.9)	26.9 (11.6-47.8)	45.7 (28.8-63.4)	87.5 (47.3-99.7)	1.29 (0.99-1.67)

Note: Data in parenthesis are 95% confidence intervals. TP = true positive, TN = true negative, FP = false positive, FN = false negative, LR + = positive likelihood ratio.

Table VII. Impact of ancillary features on observation categories, numbers, and percentages of observation categories that were identical *, upgraded ** or downgraded *** after the application of ancillary features.

			Major Features Only			
			LR-3	LR-4	LR-5	LR-M
			16	4	21	2
Major and Ancillary Features	LR-3	6	6* (14.0%)	0 (0.0%)	0 (0.0%)	0 (0.0%)
	LR-4	15	10** (23.3%)	4* (9.3%)	1*** (2.3%)	0 (0.0%)
	LR-5	20	0 (0.0%)	0 (0.0%)	20* (46.5%)	0 (0.0%)
	LR-M	2	0 (0.0%)	0 (0.0%)	0 (0.0%)	2* (4.6%)

Note: 10 hepatic observations were upgraded to LR-4 by the presence of one or more of the following ancillary features: hepatobiliary hypointensity **(n 10)**; mild-moderate T2 hyperintensity **(n 5)**; restricted diffusion **(n 4)**; intralesional fat **(n 4)**. 1 hepatic observation was downgraded to LR-4 by the presence of hepatobiliary phase isointensity. Color coding of each category is identical to conventionally used in official LI-RADS documents (9).

which the final category was upgraded due to the application of ancillary features.

Discussion

For major features, we found that nonrim APHE showed highest sensitivity (94.1%) for the diagnosis of HCC, in agreement with prior literature[16,18], with a 57.7% specificity, similarly to previously reported by Sangiovanni et al[16]. Furthermore, enhancement on arterial phase significantly correlated to the histological classification of nodules (p = 0.001), being significantly more frequent in HCCs. However, a substantial proportion of HGDNs (53.8% [7/13]) showed nonrim APHE in our series. LGDNs and most HGDNs have relatively preserved normal arterial blood supply; therefore, they usually are isoenhancing relative to liver background parenchyma on the arterial phase of CT or MR imaging[23]; nevertheless, arterial flow in some HGDNs increases owing to neoangiogenesis,

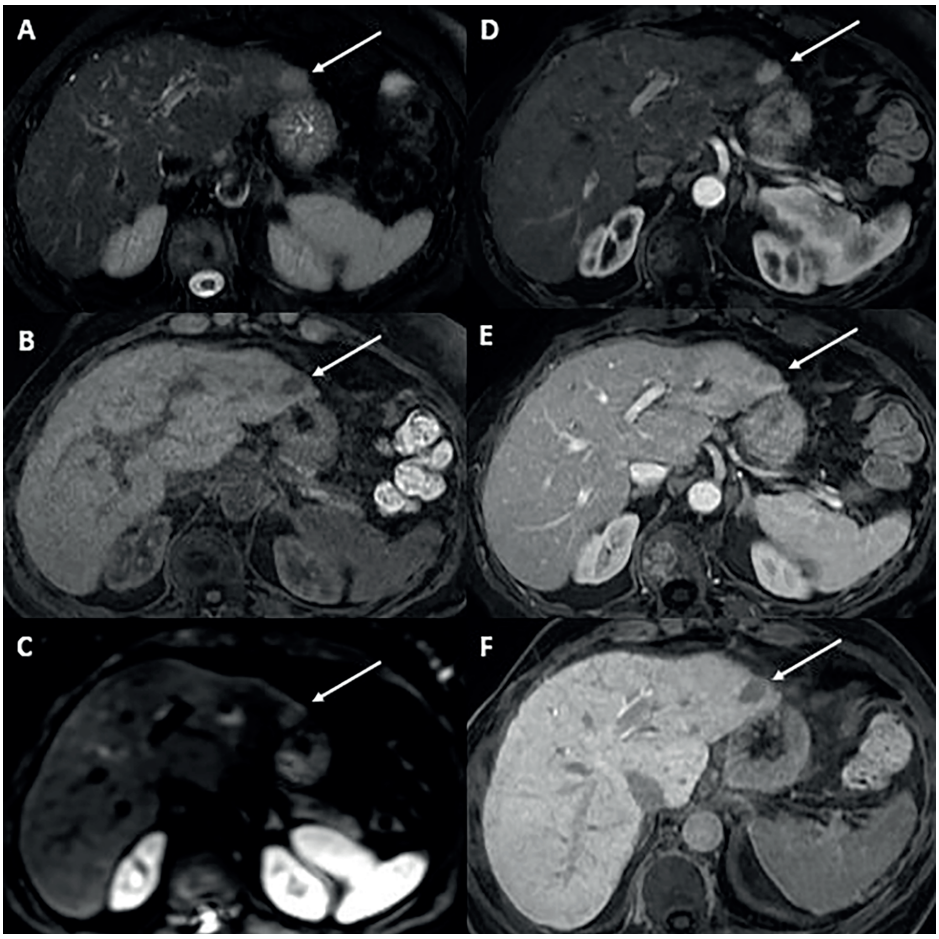

Figure 1. MR images show a liver observation measuring 18 mm in segment II with nonrim arterial phase hypenhancement and nonperipheral "washout" categorized as LR-5 according to major features of LI-RADS v2018 algorithm. (**A**) Axial T2-weighted; (**B**) Axial T1-weighted with fat saturation; (**C**) Diffusion weighted imaging; (**D**) Post-contrast arterial phase; (**E**) Post-contrast portal venous phase; (**F**) Hepatobiliary phase. The observation presents moderate T2 hyperintensity (**A**), is hypointense to the liver on the pre-contrast T1-weighted image (**B**) and shows restricted diffusion (**C**). At post-contrast imaging, the observation shows nonrim arterial phase hyperenhancement (**D**), nonperipheral "washout" (**E**) and hypointensity on hepatobiliary phase (**F**). In this case, ancillary features did not modify the LI-RADS category. Progressed hepatocellular carcinoma was confirmed with pathologic analysis after hepatectomy.

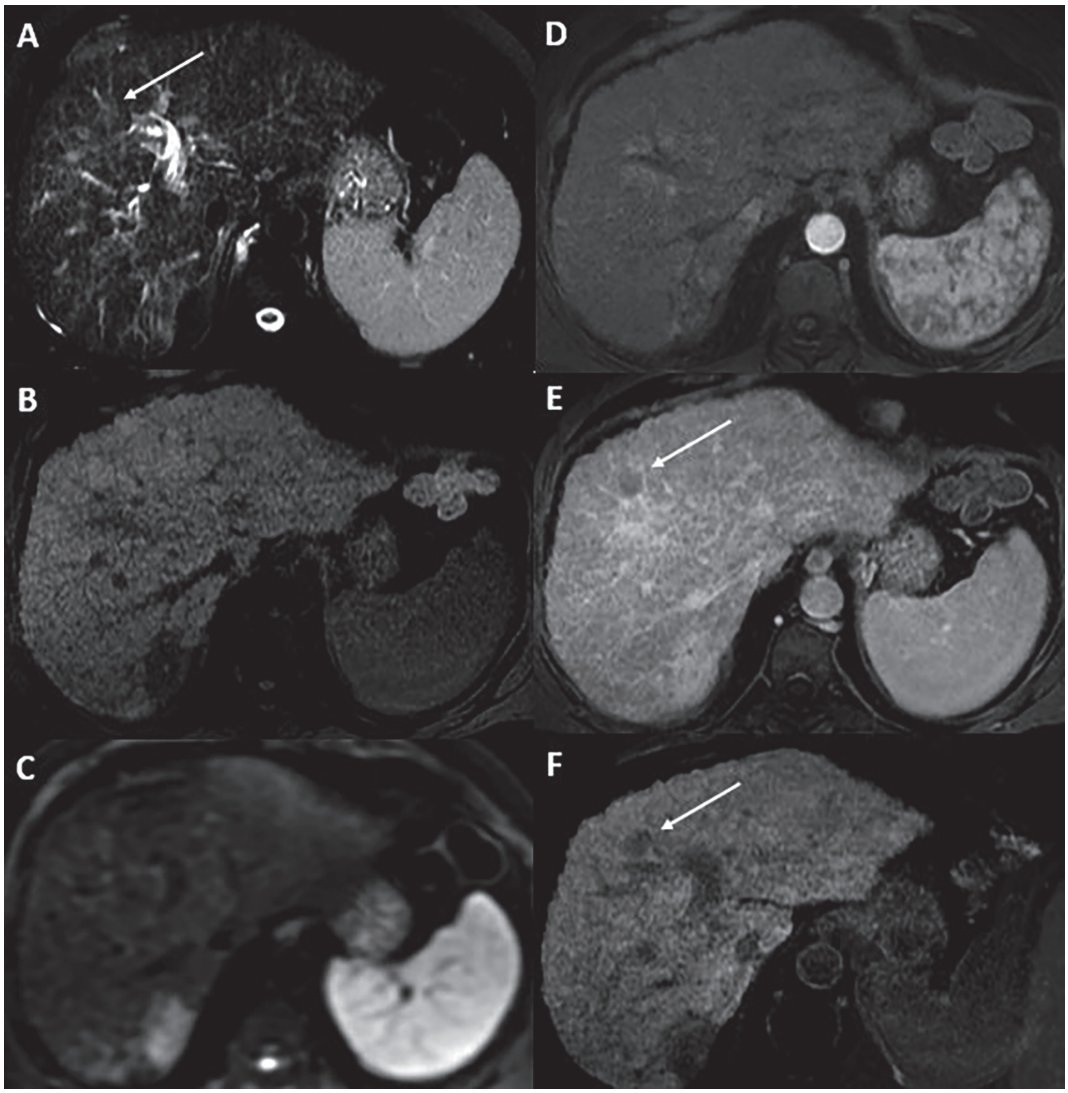

Figure 2. MR images show a liver observation measuring 19 mm in segment IV categorized as LR-3 according to LI-RADS v2018 algorithm and upgraded to LR-4 after applying ancillary features. (**A**) Axial T2-weighted; (**B**) Axial T1-weighted with fat saturation; (**C**)Diffusion weighted imaging; (**D**) Post-contrast arterial phase; (**E**) Post-contrast delayed phase; (**F**) Hepatobiliary phase. The lesion is mildly hyperintense on the T2-weighted image (arrow in **A**), isointense to the liver on the pre-contrast T1-weighted image (**B**) with no evidence of restricted diffusion (**C**). At post-contrast imaging, the observation shows no arterial phase hyperenhancement (**D**), presents nonperipheral "washout" (**E**) and is hypointense on hepatobiliary phase (**F**). In this case, ancillary features (mild T2 hyperintensity and hypointensity on hepatobiliary phase), led to category upgrade to LR-4. HGDN was confirmed with pathologic analysis after biopsy.

resulting in the potential misdiagnosis of a hypervascular HCC[24,28]. Recently, Granata et a[19] observed that most of the DNs included in their study (70% [17/24]) showed APHE. Thus, precise differentiation of HCCs and DNs based on APHE may be difficult. Moreover, we found that all of the E-HCCs (100% [6/6]) showed nonrim APHE. Although it has been reported that early, very well differentiated HCCs can be iso-hypovascular in the arterial phase[21,23] due to incomplete neoangiogenesis, Di Martino et al[29] also referred a non-negligible amount of APHE in well-differentiated HCCs included in their series (82.2% [37/45]), thus, the sensitivity of APHE for E-HCCs should still be clarified and future research is needed in this field[12].

Interestingly, we found that nonperipheral "washout" had high sensitivity (88.2%) for the diagnosis of HCCs nodules, above showed values from 59% to 79%[16,17]; however, with a 42.3%

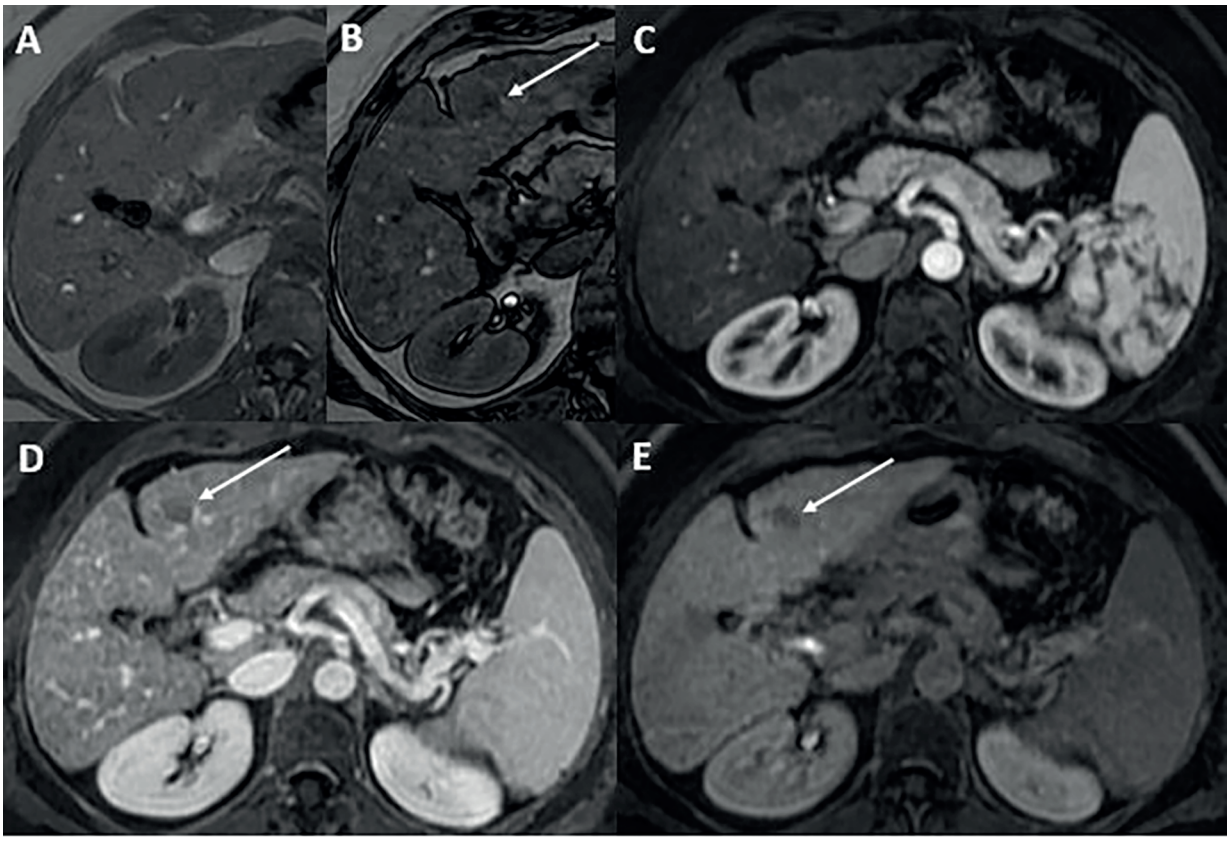

Figure 3. MR images show a liver observation measuring 12 mm in segment III categorized as LR-3 according to LI-RADS v2018 algorithm and upgraded to LR-4 after applying ancillary features. (**A**) Axial T1-weighted in-phase; (**B**) Axial T1-weighted out-of-phase; (**C**) Post-contrast arterial phase; (**D**) Post-contrast portal venous phase; (**E**) Hepatobiliary phase. The observation shows inhomogeneous signal loss in the out-of-phase image (**B**), a finding consistent with intralesional fat. At post-contrast imaging, the observation shows no arterial phase hyperenhancement (**C**), while presents nonperipheral "washout" (**D**) and hypointensity on hepatobiliary phase (**E**). In this case, ancillary features (fat in the lesion, more than adjacent liver and hypointensity on hepatobiliary phase) led to category upgrade to LR-4. LGDN was confirmed with pathologic analysis after biopsy.

specificity, lower than previously found (from 62% to 95%)[16,17]. These results can be explained by the fact that this feature was detected in a substantial proportion of DNs in our series (57.7% [15/26]). Notably, 53.8% of LGDNs (7/13), 61.5% of HGDNs (8/13), 83.3% of E-HCCs (5/6) and 90.9% of P-HCCs (10/11) showed nonperipheral "washout". Other recent studies have revealed a high percentage of DNs showing this feature; in particular, Di Martino et al[29] also indicated that washout was present in most of the DNs included in their series (89% [26/29]); additionally, Kim et al[24] found this feature in 76.5% of HGDNs (13/17). However, in the present work, we confirmed that the combination of nonrim arterial phase hyperenhancement and nonperipheral "washout" was significantly correlated to the histological classification of nodules ($p < 0.001$) and increased both specificity and PPV for the diagnosis of HCC[5-7].

Enhancing "capsule" showed a high specificity (88.5%) for HCC, in agreement with the values ranging from 86% to 96%[18,30], with a 41.2% sensitivity, similar to previously reported (42%)[18]. This feature was significantly correlated to the histological classification of nodules ($p = 0.012$) and was most frequently observed in P-HCCs (54.5% [6/11]).

Among the ancillary features in favor of malignancy in general, we confirmed the high sensitivity of hepatobiliary phase hypointensity (94.1%) for the diagnosis of HCC, in agreement with the values ranging from 75% to 95%[29,31]. However, the specificity of this feature found in our study (26.9%) was much lower than previ-

ously shown (42%-96%)[29-32]. These data can be explained by the fact that a substantial proportion of DNs (73.1% [19/26]) showed HBP hypointensity in our series. In particular, this feature was seen in 69.2% of LGDNs (9/13), 76.9% of HGDNs (10/13), 83.3% of E-HCCs (5/6), and 100% of P-HCCs (11/11) and thus, no significant difference was appreciable among the histological classification of nodules. Recently Renzulli et al[33] also verified that the specificity of HBP hypointensity for diagnosing HCCs was poor due to the high proportion of HGDNs displaying this feature; Kim et al[24] also observed HBP hypointensity in most of the HGDNs (82.4%) in their series. Similarly, we found that HBP hypointensity – as a standalone feature – provided a limited performance for differentiating HCCs from DNs, thus demonstrating that this ancillary feature may be an early event of hepatocarcinogenesis and is not a peculiar finding of HCC but may also be seen in dysplastic nodules[34].

Mild-moderate T2 hyperintensity showed moderate sensitivity (64.7%) and specificity (61.5%) for HCC, similar to values of Hecht et al[35]. This feature was observed in 30.8% of LGDNs (4/13), 46.1% of HGDNs (6/13), 50% of E-HCCs (3/6) and 72.7% of P-HCCs (8/11). Thus, although mild-moderate T2 hyperintensity did not significantly correlate to the histological classification of nodules ($p > 0.05$), it was mostly encountered in P-HCCs, in agreement with the literature[36,37].

Sensitivity and specificity of restricted diffusion were respectively of 58.8% and 65.4% for the diagnosis of HCC, much lower than previous values[19,38]. These results can be explained by the fact that none of the E-HCCs included in our series showed restricted diffusion. In particular, this ancillary feature was seen in 30.8% of LGDNs (4/13), 38.5% of HGDNs (5/13), and 90.9% of P-HCCs (10/11). Some studies[38-41] supported the utility of diffusion weighted imaging (DWI) in diagnosing HCC[39], especially when combined with dynamic post-contrast findings[40,41] or HBP hypointensity[38]. Nevertheless, other papers documented only moderate to no added value of DWI compared with conventional MR imaging[42,43], as some HCCs, particularly those with well-differentiated components, may show no or minimal restricted diffusion[43]. Kim at al[24] reported that restricted diffusion was present in a low percentage of E-HCCs (21%) included in their series. In our study population, restricted diffusion had moderate sensitivity and specificity – as a standalone feature – for the diagnosis of HCC, nevertheless, was significantly more frequent in P-HCCs ($p = 0.001$), likely reflecting higher histological tumor grading[44,45].

Fat in a mass, more than in the adjacent liver, was observed in 11.8% of HCCs, with a specificity of 76.9%, consistent with the literature[17,18]. However, we encountered intralesional fat in 23.1% of DNs (6/26), 5 of which were LGDNs. Therefore, in our study, fat in mass was not significantly correlated to histological classification of nodules. The contribution of the ancillary feature to overall diagnostic performance hence is limited because fat in a mass, more than in background liver, does not allow reliable distinction of E-HCCs from high-grade and even LGDNs and may coexist in P-HCCs[18].

For LI-RADS category indicating definitely HCC (LR-5), interpretation that included ancillary features did not remarkably modify sensitivity and specificity compared with categorization according to major features only. In fact upgrade from LR-4 to LR-5 category is not permitted by LI-RADS. Furthermore, in our study, the category was downgraded in 1 of 41 observations eligible for category downgrade (2.4%) and in particular, it was downgraded to LR4 in 1 of 21 LR-5 observations (4.7%). Thus, we did not observe a notable impact of ancillary features on LR-5 category diagnostic performance. The present work certifies confirms that LR-5 category provides high specificity for the diagnosis of HCC; nevertheless, the specificity that we observed was lower than the near-perfect values previously stated (89.9%-97.1%)[26,27]. These discrepancies are probably due to our study series which, was strictly limited to small observations (≤ 2 cm) and did not include LR-1/LR-2 and LR-TIV observations.

Additionally, when combining LI-RADS categories indicating probably HCC or definitely HCC (LR-4, LR-5), we observed that sensitivity improved from 88.2% to 94.1% at both interpretations (i.e., including or not ancillary features). However, specificity was poor, and notably, the interpretation that included ancillary features further decreased specificity for HCC (from 80.8% to 26.9%) compared with categorization according to major features only (from 76.9% to 65.4%).

The value of ancillary features favoring malignancy (including ancillary features favoring HCC in particular) to upgrade LR-3 observations is controversial in literature, as well the combination of LR-4 and LR-5 to diagnose HCC. Recently

Cerny et al[27] remarked that, the use of ancillary features to upgrade LR-3 observations to LR-4 increased sensitivity for HCC (from 76% to 88%), while preserved high specificity (from 88% to 86%) for the combination of LR-4, LR-5 and LR-5V (equivalent of LR-TIV in version 2018). In a separate study Ronot et al[26], combined LR-4 with LR-5/LR-5V, and the sensitivity increased (from 72.5% to 87%) but the specificity decreased (from 89.9% to 69%) at MRI. Moreover, in the same work[26], the use of ancillary features favoring malignancy (including ancillary features favoring HCC in particular) to upgrade LR-3 observations to LR-4 increased sensitivity for HCC (from 87% to 97%), but further reduced specificity (from 69% to 51%) at MRI. Our findings are similar to the latter study. Although LR-TIV observations were not included in our series, we observed that the combination of LR-4 and LR-5 for the diagnosis of HCC markedly increased the sensitivity for both interpretations (i.e., before and after application of ancillary features), but resulted in an unacceptably low specificity, especially when applying ancillary features (26.9%). Therefore, as Ronot et al[26] we strongly believe that LR-4 and LR-5 categories should not be combined for the diagnosis of HCC. Our results can be explained by the fact that the application of ancillary features increased the proportion of LR-4 observations that were confirmed to be DNs at pathologic analysis. Prior works assessing the clinical application of ancillary features have shown that their use modifies the final category in 15-35% of observations[13,27,46], with about 63% of LR-4 observations being upgraded from LR-3. Similarly, we discovered that application of ancillary features modified the final category in 25.6% of observations (11/43), predominantly upgraded from LR-3 to LR-4 (10/11), with 66.7% of LR-4 observations (10/15) being upgraded from LR-3. Of note, all of the observations that were upgraded from LR-3 to LR-4 by using ancillary features in combination with major features were confirmed to be DNs (10/10, of which 5 were LGDNs, and 5 were HGDNs). Thus, although, DNs are not clearly classified in a particular LI-RADS category[47,48], we detected that the use of ancillary features increased the overall proportion of DNs categorized as LR-4 (from 11.5% to 53.8%, respectively), and in particular, we found that not merely HGDNs were frequently categorized as LR-4 by using ancillary features (46.1%), similarly to that reported by Kim et al[24], but also LGDNs were mostly categorized as LR-4 with their application (61.5%).

Recently, it has been shown that a minority of LR-4 observations progress to LR-5; nevertheless, it has been reported that cumulative incidence of progression to a malignant category is higher for LR-4 observations than for LR-3 observations[49]. Therefore, our data suggest that the application of ancillary features may be used to adapt patient management in LR-4 observations, prompting close follow up or even a more aggressive approach, including liver biopsy. Indeed, this approach should be validated on a large scale. However, further work is needed to assess the incremental benefit of these features for LI-RADS categorization, as well studies are needed to define the optimal workup strategy of LR-4 observations, as it is still unclear if they should undergo biopsy[50]. In this regard, the role of multidisciplinary management is pivotal to achieve a tailored workup of each patient.

Our study had some limitations. First, the retrospective nature of the study, as well as the application of a strict requirement of pathologic proof as reference standard for all observations, imply the possibility of selection bias. Second, although, all observations were pathologically proven, sampling error or mistargeting may have decreased the reliability of the histological diagnosis for those lesions that only underwent FNB/CNB, as shown by one LR-M observation included in our series which was confirmed being an LGDN at FNB. Third, the number of investigated lesions was relatively small, thus, we were not able to compute the diagnostic performance for some infrequently observed features. Moreover, as clinical practice guidelines do not mandate pathologic proof for observations that meet their imaging criteria for HCC[5-7], this contributed to restricting our study to a small number of observations, some of which were reasonably considered atypical from a radiological point of view. This context this could explain the high percentage of LGDNs displaying HBP hypointensity in our series. Therefore, further investigation on a larger series of cases is needed to assess diagnostic performance and clinical application of major and ancillary features in differentiating HCC from DNs in at-risk patients. Fourth, we did not compute diagnostic performance of ancillary features favoring benignity, as they were infrequently observed in our series. Nevertheless, when assigning LI-RADS v2018 category at imaging analysis, the presence of hepatobiliary phase isointensity was taken in count by the two revising radiologists

and determined downgrade in one of 41 observations eligible for category downgrade, thus not affecting diagnostic performance of LR-5 and the combination of LR-4, LR-5 categories. Finally, the evaluation of MR images by two radiologists in consensus, gave no data about the interobserver agreement, reducing the ability to make conclusive statements concerning accuracy.

Conclusions

The results of our study of diagnostic performance suggest that LI-RADS major features have moderate to high specificity for diagnosing small HCCs, except for nonperipheral "washout". When considered in combination, nonrim APHE and nonperipheral "washout" more significantly correlate to the histological classification of nodules providing higher specificity and PPV for HCC in at-risk patients, than when considered as stand-alone features. LI-RADS ancillary features in favor of malignancy – or HCC in particular – have moderate to low specificity, providing limited value for non-invasive diagnosis of small HCCs. Notably, none of the ancillary features favoring malignancy – or HCC in particular – were observed significantly more often in HCCs than in DNs, except for restricted diffusion in P-HCCs. Thus, they cannot reliably discriminate small observations in at-risk patients, and precise differentiation of preneoplastic lesions may be uncertain due to the overlap of imaging findings. However, the application of ancillary features modified the final category in a substantial proportion of observations from LR-3 to LR-4, increasing the overall proportion of dysplastic nodules categorized as LR-4. This approach may be used to allow possible changes in the management of these patients. Finally, regarding the diagnostic performance of LI-RADS categories, our results show that the highest sensitivity for HCC is observed with the combination of LR-4 and LR-5 categories, in contrast, higher specificity is provided with LR-5 alone.

Conflict of Interest

The Authors declare that they have no conflict of interests.

Acknowledgements

The authors of this manuscript state that this work has not received any funding. Institutional Review Board approval was obtained and written informed consent from the patients was waived by the Institutional Review Board. Methodology: retrospective, performed at one institution.

References

1) Mittal S, El-Serag HB. Epidemiology of hepatocellular carcinoma: consider the population. J Clin Gastroenterol 2013; 47 Suppl: S2-6.
2) Park YN. Update on precursor and early lesions of hepatocellular carcinomas. Arch Pathol Lab Med 2011; 135: 704-715.
3) Hytiroglou P, Park YN, Krinsky G, Theise ND. Hepatic precancerous lesions and small hepatocellular carcinoma. Gastroenterol Clin North Am 2007; 36: 867-887, vii.
4) International Consensus Group for Hepatocellular Neoplasia. The International Consensus Group for Hepatocellular Neoplasia. Pathologic diagnosis of early hepatocellular carcinoma: a report of the International Consensus Group for Hepatocellular Neoplasia. Hepatology 2009; 49: 658-664.
5) Heimbach JK, Kulik LM, Finn RS, Sirlin CB, Abecassis MM, Roberts LR, Zhu AX, Murad MH, Marrero JA. AASLD guidelines for the treatment of hepatocellular carcinoma. Hepatology 2018; 67: 358-380.
6) European Association for the Study of the Liver. Electronic address: easloffice@easloffice.eu, European Association for the Study of the Liver. EASL Clinical Practice Guidelines: Management of hepatocellular carcinoma. J Hepatol 2018; 69: 182-236.
7) Policies – OPTN [Internet]. [cited 2019 Jul 17]. Available from: https://optn.transplant.hrsa.gov/governance/policies/
8) Tang A, Cruite I, Mitchell DG, Sirlin CB. Hepatocellular carcinoma imaging systems: why they exist, how they have evolved, and how they differ. Abdom Radiol (N Y) 2018; 43: 3-12.
9) LI-RADS [Internet]. [cited 2019 Jul 17]. Available from: https://www.acr.org/Clinical-Resources/Reporting-and-Data-Systems/LI-RADS
10) Marrero JA, Kulik LM, Sirlin CB, Zhu AX, Finn RS, Abecassis MM, Roberts LR, Heimbach JK. Diagnosis, staging, and management of hepatocellular carcinoma: 2018 Practice Guidance by the American Association for the Study of Liver Diseases. Hepatology 2018; 68: 723-750.
11) van der Pol CB, Lim CS, Sirlin CB, McGrath TA, Salameh JP, Bashir MR, Tang A, Singal AG, Costa AF, Fowler K, McInnes MDF. Accuracy of the liver imaging reporting and data system in computed tomography and magnetic resonance image analysis of hepatocellular carcinoma or overall malignancy-A systematic review. Gastroenterology 2019; 156: 976-986.
12) Tang A, Bashir MR, Corwin MT, Cruite I, Dietrich CF, Do RKG, Ehman EC, Fowler KJ, Hussain HK, Jha RC,

Karam AR, Mamidipalli A, Marks RM, Mitchell DG, Morgan TA, Ohliger MA, Shah A, Vu KN, Sirlin CB; LI-RADS Evidence Working Group. Evidence supporting LI-RADS major features for CT- and MR imaging-based diagnosis of hepatocellular carcinoma: a systematic review. Radiology 2018; 286: 29-48.

13) Choi SH, Byun JH, Kim SY, Lee SJ, Won HJ, Shin YM, Kim PN. Liver imaging reporting and data system v2014 with gadoxetate disodium-enhanced magnetic resonance imaging: validation of LI-RADS category 4 and 5 criteria. Invest Radiol 2016; 51: 483-490.

14) Fraum TJ, Tsai R, Rohe E, Ludwig DR, Salter A, Nalbantoglu I, Heiken JP, Fowler KJ. Differentiation of hepatocellular carcinoma from other hepatic malignancies in patients at risk: diagnostic performance of the liver imaging reporting and data system version 2014. Radiology 2018; 286: 158-172.

15) Forner A, Vilana R, Ayuso C, Bianchi L, Solé M, Ayuso JR, Boix L, Sala M, Varela M, Llovet JM, Brú C, Bruix J. Diagnosis of hepatic nodules 20 mm or smaller in cirrhosis: prospective validation of the noninvasive diagnostic criteria for hepatocellular carcinoma. Hepatology 2008; 47: 97-104. Erratum in: Hepatology 2008; 47: 769.

16) Sangiovanni A, Manini MA, Iavarone M, Romeo R, Forzenigo LV, Fraquelli M, Massironi S, Della Corte C, Ronchi G, Rumi MG, Biondetti P, Colombo M. The diagnostic and economic impact of contrast imaging techniques in the diagnosis of small hepatocellular carcinoma in cirrhosis. Gut 2010; 59: 638-644.

17) Kim TK, Lee KH, Jang HJ, Haider MA, Jacks LM, Menezes RJ, Park SH, Yazdi L, Sherman M, Khalili K. Analysis of gadobenate dimeglumine-enhanced MR findings for characterizing small (1-2-cm) hepatic nodules in patients at high risk for hepatocellular carcinoma. Radiology 2011; 259: 730-738.

18) Rimola J, Forner A, Tremosini S, Reig M, Vilana R, Bianchi L, Rodríguez-Lope C, Solé M, Ayuso C, Bruix J. Non-invasive diagnosis of hepatocellular carcinoma ≤ 2 cm in cirrhosis. Diagnostic accuracy assessing fat, capsule and signal intensity at dynamic MRI. J Hepatol 2012; 56: 1317-1323.

19) Granata V, Fusco R, Avallone A, Filice F, Tatangelo F, Piccirillo M, Grassi R, Izzo F, Petrillo A. Critical analysis of the major and ancillary imaging features of LI-RADS on 127 proven HCCs evaluated with functional and morphological MRI: lights and shadows. Oncotarget 2017; 8: 51224-51237.

20) Bartolozzi C, Battaglia V, Bargellini I, Bozzi E, Campani D, Pollina LE, Filipponi F. Contrast-enhanced magnetic resonance imaging of 102 nodules in cirrhosis: correlation with histological findings on explanted livers. Abdom Imaging 2013; 38: 290-296.

21) Sano K, Ichikawa T, Motosugi U, Sou H, Muhi AM, Matsuda M, Nakano M, Sakamoto M, Nakazawa T, Asakawa M, Fujii H, Kitamura T, Enomoto N, Araki T. Imaging study of early hepatocellular carcinoma: usefulness of gadoxetic acid-enhanced MR imaging. Radiology 2011; 261: 834-844.

22) Inoue T, Kudo M, Komuta M, Hayaishi S, Ueda T, Takita M, Kitai S, Hatanaka K, Yada N, Hagiwara S, Chung H, Sakurai T, Ueshima K, Sakamoto M, Maenishi O, Hyodo T, Okada M, Kumano S, Murakami T. Assessment of Gd-EOB-DTPA-enhanced MRI for HCC and dysplastic nodules and comparison of detection sensitivity versus MDCT. J Gastroenterol 2012; 47: 1036-1047.

23) Park HJ, Choi BI, Lee ES, Park SB, Lee JB. How to differentiate borderline hepatic nodules in hepatocarcinogenesis: emphasis on imaging diagnosis. Liver Cancer 2017; 6: 189-203.

24) Kim BR, Lee JM, Lee DH, Yoon JH, Hur BY, Suh KS, Yi NJ, Lee KB, Han JK. Diagnostic performance of gadoxetic acid-enhanced liver MR imaging versus multidetector CT in the detection of dysplastic nodules and early hepatocellular carcinoma. Radiology 2017; 285: 134-146.

25) Inchingolo R, Faletti R, Grazioli L, Tricarico E, Gatti M, Pecorelli A, Ippolito D. MR with Gd-EOB-DTPA in assessment of liver nodules in cirrhotic patients. World J Hepatol 2018; 10: 462-473.

26) Ronot M, Fouque O, Esvan M, Lebigot J, Aubé C, Vilgrain V. Comparison of the accuracy of AASLD and LI-RADS criteria for the non-invasive diagnosis of HCC smaller than 3 cm. J Hepatol 2018; 68: 715-723.

27) Cerny M, Bergeron C, Billiard JS, Murphy-Lavallée J, Olivié D, Bérubé J, Fan B, Castel H, Turcotte S, Perreault P, Chagnon M, Tang A. LI-RADS for MR imaging diagnosis of hepatocellular carcinoma: performance of major and ancillary features. Radiology 2018; 288: 118-128.

28) Hayashi M, Matsui O, Ueda K, Kawamori Y, Gabata T, Kadoya M. Progression to hypervascular hepatocellular carcinoma: correlation with intranodular blood supply evaluated with CT during intraarterial injection of contrast material. Radiology 2002; 225: 143-149.

29) Di Martino M, Anzidei M, Zaccagna F, Saba L, Bosco S, Rossi M, Ginanni Corradini S, Catalano C. Qualitative analysis of small (≤2 cm) regenerative nodules, dysplastic nodules and well-differentiated HCCs with gadoxetic acid MRI. BMC Med Imaging 2016; 16: 62.

30) Khan AS, Hussain HK, Johnson TD, Weadock WJ, Pelletier SJ, Marrero JA. Value of delayed hypointensity and delayed enhancing rim in magnetic resonance imaging diagnosis of small hepatocellular carcinoma in the cirrhotic liver. J Magn Reson Imaging 2010; 32: 360-366.

31) Orlacchio A, Chegai F, Fabiano S, Merolla S, Funel V, Di Giuliano F, Manuelli M, Tisone G, Francioso S, Angelico M, Palmieri G, Simonetti G. Role of MRI with hepatospecific contrast agent in the identification and characterization of focal liver lesions: pathological correlation in explanted livers. Radiol Med 2016; 121: 588-596.

32) Lee MH, Kim SH, Park MJ, Park CK, Rhim H. Gadoxetic acid-enhanced hepatobiliary phase MRI and high-b-value diffusion-weighted imaging to distinguish well-differentiated hepatocellular carcino-

mas from benign nodules in patients with chronic liver disease. AJR Am J Roentgenol 2011; 197: W868-875.

33) Renzulli M, Biselli M, Brocchi S, Granito A, Vasuri F, Tovoli F, Sessagesimi E, Piscaglia F, D'Errico A, Bolondi L, Golfieri R. New hallmark of hepatocellular carcinoma, early hepatocellular carcinoma and high-grade dysplastic nodules on Gd-EOB-DTPA MRI in patients with cirrhosis: a new diagnostic algorithm. Gut 2018; 67: 1674-1682.

34) Kogita S, Imai Y, Okada M, Kim T, Onishi H, Takamura M, Fukuda K, Igura T, Sawai Y, Morimoto O, Hori M, Nagano H, Wakasa K, Hayashi N, Murakami T. Gd-EOB-DTPA-enhanced magnetic resonance images of hepatocellular carcinoma: correlation with histological grading and portal blood flow. Eur Radiol 2010; 20: 2405-2413.

35) Hecht EM, Holland AE, Israel GM, Hahn WY, Kim DC, West AB, Babb JS, Taouli B, Lee VS, Krinsky GA. Hepatocellular carcinoma in the cirrhotic liver: gadolinium-enhanced 3D T1-weighted MR imaging as a stand-alone sequence for diagnosis. Radiology 2006; 239: 438-447.

36) Choi JY, Lee JM, Sirlin CB. CT and MR imaging diagnosis and staging of hepatocellular carcinoma: part II. Extracellular agents, hepatobiliary agents, and ancillary imaging features. Radiology 2014; 273: 30-50.

37) Hussain HK, Syed I, Nghiem HV, Johnson TD, Carlos RC, Weadock WJ, Francis IR. T2-weighted MR imaging in the assessment of cirrhotic liver. Radiology 2004; 230: 637-644.

38) Inchingolo R, De Gaetano AM, Curione D, Ciresa M, Miele L, Pompili M, Vecchio FM, Giuliante F, Bonomo L. Role of diffusion-weighted imaging, apparent diffusion coefficient and correlation with hepatobiliary phase findings in the differentiation of hepatocellular carcinoma from dysplastic nodules in cirrhotic liver. Eur Radiol 2015; 25: 1087-1096.

39) Piana G, Trinquart L, Meskine N, Barrau V, Beers BV, Vilgrain V. New MR imaging criteria with a diffusion-weighted sequence for the diagnosis of hepatocellular carcinoma in chronic liver diseases. J Hepatol 2011; 55: 126-132.

40) Xu PJ, Yan FH, Wang JH, Lin J, Ji Y. Added value of breathhold diffusion-weighted MRI in detection of small hepatocellular carcinoma lesions compared with dynamic contrast-enhanced MRI alone using receiver operating characteristic curve analysis. J Magn Reson Imaging 2009; 29: 341-349.

41) Vandecaveye V, De Keyzer F, Verslype C, Op de Beeck K, Komuta M, Topal B, Roebben I, Bielen D, Roskams T, Nevens F, Dymarkowski S. Diffusion-weighted MRI provides additional value to conventional dynamic contrast-enhanced MRI for detection of hepatocellular carcinoma. Eur Radiol 2009; 19: 2456-2466.

42) Park MS, Kim S, Patel J, Hajdu CH, Do RK, Mannelli L, Babb JS, Taouli B. Hepatocellular carcinoma: detection with diffusion-weighted versus contrast-enhanced magnetic resonance imaging in pretransplant patients. Hepatology 2012; 56: 140-148.

43) Kim YK, Kim CS, Han YM, Lee YH. Detection of liver malignancy with gadoxetic acid-enhanced MRI: is addition of diffusion-weighted MRI beneficial? Clin Radiol 2011; 66: 489-496.

44) Taouli B, Koh DM. Diffusion-weighted MR imaging of the liver. Radiology 2010; 254: 47-66.

45) Nakanishi M, Chuma M, Hige S, Omatsu T, Yokoo H, Nakanishi K, Kamiyama T, Kubota K, Haga H, Matsuno Y, Onodera Y, Kato M, Asaka M. Relationship between diffusion-weighted magnetic resonance imaging and histological tumor grading of hepatocellular carcinoma. Ann Surg Oncol 2012; 19: 1302-1309.

46) Joo I, Lee JM, Lee DH, Ahn SJ, Lee ES, Han JK. Liver imaging reporting and data system v2014 categorization of hepatocellular carcinoma on gadoxetic acid-enhanced MRI: comparison with multiphasic multidetector computed tomography. J Magn Reson Imaging 2017; 45: 731-740.

47) Narsinh KH, Cui J, Papadatos D, Sirlin CB, Santillan CS. Hepatocarcinogenesis and LI-RADS. Abdom Radiol (NY) 2018; 43: 158-168.

48) Shah A, Tang A, Santillan C, Sirlin C. Cirrhotic liver: what's that nodule? The LI-RADS approach. J Magn Reson Imaging 2016; 43: 281-294.

49) Tanabe M, Kanki A, Wolfson T, Costa EA, Mamidipalli A, Ferreira MP, Santillan C, Middleton MS, Gamst AC, Kono Y, Kuo A, Sirlin CB. Imaging outcomes of Liver Imaging Reporting and Data System version 2014 category 2, 3, and 4 observations detected at CT and MR imaging. Radiology 2016; 281: 129-139.

50) Chernyak V, Fowler KJ, Kamaya A, Kielar AZ, Elsayes KM, Bashir MR, Kono Y, Do RK, Mitchell DG, Singal AG, Tang A, Sirlin CB. Liver Imaging Reporting and Data System (LI-RADS) version 2018: imaging of hepatocellular carcinoma in at-risk patients. Radiology 2018; 289: 816-830.